

Effect of Hydrostatic Confining Pressure on the Failure Mode and Compressive Strength of Polycrystalline Ice[†]

Yukiko Mizuno

Institute of Low Temperature Science, Hokkaido University, Kita 19 Nishi 8, Kitaku, Sapporo 060, Japan

Received: October 11, 1996; In Final Form: November 3, 1997[⊗]

Compressive tests were performed on fine and coarse-grained granular ice with grain size of 1 and 10 mm and coarse-grained columnar ice at strain rates from 3×10^{-4} to $5 \times 10^{-2} \text{ s}^{-1}$ under hydrostatic confining pressure from 0.1 to 50 MPa, at $-11 \pm 0.5 \text{ }^{\circ}\text{C}$. The effect of hydrostatic confining pressure on the failure mode and the compressive strength were examined with reference to grain size and strain rate. At a constant strain rate, the compressive fracture/yield stress increased with increasing confining pressure up to a critical confining pressure at which the stress attains a maximum and the process of failure changes from brittle to ductile. Above the critical confining pressure, the compressive stress was not changed by confining pressure at lower strain rates, while it decreased at higher strain rates as the confining pressure increased. The critical confining pressure increased with increase in strain rate and grain size. A higher confining pressure was required to inhibit brittle failure for columnar ice and coarse-grained granular ice than for fine-grained granular ice at the same strain rate. Application of a confining pressure above 20 MPa caused fine-grain ice to deform in a ductile manner for the strain rate applied; a confining pressure of 50 MPa was required at $2.5 \times 10^{-2} \text{ s}^{-1}$ for coarse-grained granular ice and $1 \times 10^{-2} \text{ s}^{-1}$ for columnar ice. The correlation between the deformation behavior and the change in the internal structure was examined.

1. Introduction

Polycrystalline ice under loading changes from ductile to brittle as the strain rate increases. The compressive strength of ice increases with increase in strain rate and reaches a maximum at a critical strain rate at which a brittle to ductile transition occurs.¹ The maximum unconfined compressive strength of polycrystalline ice with randomly oriented small grains of about 1 mm is at most 10 MPa at a critical strain rate of around 10^{-4} s^{-1} at $-10 \text{ }^{\circ}\text{C}$.² As ice in the natural environment suffers a certain degree of confinement, the deformation behavior and the mechanical strength are expected to be different from those of ice without confinement.

There have been many studies on the mechanical behavior of confined ice with interest in both ice physics and practical engineering. Haefeli et al.,³ Jones and Chew,⁴ and Mizuno⁵ performed compressive creep experiments combined with hydrostatic confining pressure and showed the effect of confining pressure on plastic deformation in relation to the melting point depression, activation volume, and microprocess in the crystal texture. A further study was conducted by Jones⁶ on the effect of confining pressure on the compressive strength of granular ice over a wide range of strain rate and hydrostatic confining pressure associated with both creep and brittle behavior. He showed that the difference in strength between the confined and unconfined stress tests was little at strain rates below 10^{-6} s^{-1} , while above $5 \times 10^{-3} \text{ s}^{-1}$ it increased with further increase in strain rate. Kalifa et al.⁷ carried out compression tests on granular ice combined with the hydrostatic confining pressures of up to 10 MPa at strain rates from 7×10^{-6} to $5 \times 10^{-3} \text{ s}^{-1}$ in order to study the role of microcracking

on failure in the ductile to brittle transition zone and the effects of confining pressure and strain rate on crack population, as well as on strength and strain at the peak stress. Rist et al.⁸ performed compressive tests on granular ice at a strain rate of 10^{-2} s^{-1} under hydrostatic confining pressures of up to 20 MPa and examined the relationship between microcracking and strength. Similar tests conducted by Rist and Murrel⁹ under a wide range of hydrostatic confining pressure and at lower temperatures demonstrated the effects of confining pressure and temperature on the failure mode, strength, and failure process in connection with microcracking. Schulson et al.,¹⁰ Smith and Schulson,¹¹ and Weiss and Schulson¹² conducted experiments on the brittle failure of granular and columnar ice under nonhydrostatic confinement but multiaxial compressive loading between solid platens. They examined the failure stress, failure mode, and internal cracking as a function of confinement ratio, emphasizing the frictional crack-sliding/wing-crack mechanism in brittle failure.

In the present study we gave special attention to the microprocesses associated with the macroscopic deformation characterized by the strength and the failure mode. We performed compressive tests on fine ($\sim 1 \text{ mm}$) and coarse ($\sim 10 \text{ mm}$) grained granular ice and coarse (across column $\sim 10 \text{ mm}$) columnar ice under hydrostatic confining pressures of up to 50 MPa and at strain rates in the range 3×10^{-4} to $5 \times 10^{-2} \text{ s}^{-1}$. Effects of confining pressure, grain size, and strain rate on the failure mode and the strength were examined.

2. Sample Preparation

Fine-grained, homogeneously oriented polycrystalline ice with a grain size of about 1 mm in diameter was obtained by freezing an aggregation of snow particles saturated with degassed and distilled water. It had a density of 0.905 Mg m^{-3} and contained small air bubbles of several tens of micrometers in diameter,

[†] Originally submitted for inclusion in the Physics and Chemistry of Ice issue of *J. Phys. Chem. B* (1997, 101, 6079–6312).

[⊗] Abstract published in *Advance ACS Abstracts*, December 15, 1997.

mostly at grain boundaries. The coarse-grained granular samples were prepared as follows. First, a number of ice cubes about 10 mm on edge were cut from a block of columnar ice and placed in a container that was filled with distilled water of temperature slightly higher than the melting point. After the corners of the ice cube had melted slightly, the mixture of ice cubes and water was frozen at $-10\text{ }^{\circ}\text{C}$. The coarse-grained granular sample had a density of 0.910 Mg m^{-3} and air bubbles at grain boundaries that were much smaller in number but larger in size than those in the fine grained ice. The columnar ice was made by downward freezing of water in a container ($0.3\text{ m} \times 0.3\text{ m} \times 0.3\text{ m}$) with insulated sides and bottom. Freezing was initiated by covering the surface with ice grains of about 6 mm in diameter to control the size of the columnar grains. This procedure made S-2 type columnar ice with a grain size of 8–9 mm in diameter and several tens of millimeters long. We performed *c*-axis analysis on columnar ice specimens by the X-ray Laue method and determined the type of columnar ice.

Cylindrical specimens 37–40 mm in diameter and 60–65 mm in length were prepared with a lathe. The columnar ice was machined so as to have the cylindrical axis either along or across the columnar grains. A sufficient annealing time of more than 1 week was given before a test to eliminate possible mechanical damage during sample preparation.

Compressive tests were conducted on 52 samples of fine-grained granular ice, 24 of coarse-grained granular ice, and 81 of columnar ice.

3. Method

The tests were carried out in a high-pressure cell designed in our laboratory and mounted in a testing machine (Instron model 4204). Details of the high-pressure cell are given in Mizuno.⁵ The testing system was placed in a cold room at $-11\text{ }^{\circ}\text{C}$ controlled within $\pm 0.5\text{ }^{\circ}\text{C}$; the temperature of the pressure cell was regulated separately to an accuracy of $\pm 0.1\text{ }^{\circ}\text{C}$. Hydrostatic pressure was applied by a manually operated pump to a fixed pressure within, at most, 30 min and kept constant during a test. The specimens were sealed in a thin rubber jacket together with end caps to isolate them from the pressurized oil. Compressive loads were applied to the samples along the cylinder axis through a loading piston at a nominally constant rate of cross-head motion. The tests were carried out at strain rates from 3×10^{-4} to $5 \times 10^{-2}\text{ s}^{-1}$ for fine-grained granular ice and from 1×10^{-3} to $5 \times 10^{-2}\text{ s}^{-1}$ for coarse-grained granular and columnar ice. The load–time curves were recorded on a standard Instron chart recorder for strain rate less than $1 \times 10^{-2}\text{ s}^{-1}$. Above that, the curves were recorded on an oscillographic recorder with a response time of $10\text{ }\mu\text{s}$ and a memory for storage of the measurements. We did not measure the strain directly by use of strain gauge, and the load–time curves were converted to nominal stress–strain curves using the cross-head displacement rates.

4. Results

4.1. Stress–Strain Curve. Figure 1A shows stress–strain curves for various confining pressure for fine-grained granular ice obtained at a strain rate of $1 \times 10^{-2}\text{ s}^{-1}$ at $-11 \pm 0.5\text{ }^{\circ}\text{C}$. The unconfined brittle strength of about 6 MPa increased to 22.5 MPa at the confining pressure of 5 MPa, at which the deformation behavior was ductile. As is evident from the figure, the highest stress at this strain rate was obtained with a confining pressure of 5 MPa. The strength decreased and the strain at the peak stress increased with further increase in confining pressure.

Typical stress–strain curves at $5 \times 10^{-2}\text{ s}^{-1}$ are shown in Figure 1B for various confining pressures. At this strain rate, brittle failure occurred by shear under confining pressures of 5 and 10 MPa, while deformation was ductile for a confining pressure of 20 MPa. The maximum strength at this strain rate was obtained with a confining pressure of 20 MPa, and the strength decreased with further increase in confining pressure. The relation between compressive fracture/yield strength of fine-grained ice and hydrostatic confining pressure for various strain rates are summarized in Figure 1C. The stress for brittle fracture at higher strain rates and/or low confinement varied; each value plotted is the average of three measurements. The compressive strength increased with increasing hydrostatic pressure to a critical confining pressure. Above that, the strength changed little with confining pressure at lower strain rate ($3 \times 10^{-4}\text{ s}^{-1}$, $3 \times 10^{-3}\text{ s}^{-1}$), while it decreased at higher strain rate ($1 \times 10^{-2}\text{ s}^{-1}$, $5 \times 10^{-2}\text{ s}^{-1}$) with further increase in confining pressure. At the strain rates shown in Figure 1C, the unconfined brittle strength varied between 3 and 7 MPa regardless of strain rate. A confining pressure of 5 MPa was sufficient to suppress brittle fracture at strain rates of 3×10^{-4} and $3 \times 10^{-3}\text{ s}^{-1}$, allowing the strength to increase under the ductile behavior. At these two strain rates the effect of confining pressure on yield stress was remarkable below 10 MPa, while the stress changed little with further increase in confining pressure. Even at a strain rate of $1 \times 10^{-2}\text{ s}^{-1}$, a confining pressure of 5 MPa allowed ice to deform in a ductile manner and the strength to rise steeply to a value of 23 MPa. In contrast with the lower strain rates, the strength decreased with further increase in confining pressure. At the highest strain rate ($5 \times 10^{-2}\text{ s}^{-1}$), shear fracture occurred under confining pressures of 5 and 10 MPa and the fracture strength at 10 MPa was slightly larger than that for 5 MPa. A brittle to ductile transition at this strain rate occurred for the confining pressure of 20 MPa, and above that the yield stress decreased with increasing confining pressure. Here we have distinguished between ductile and brittle behavior using the stress–strain curves. As can be seen in Figure 1C, the effect of confining pressure on the strength was remarkable as the strain rate increased. For fine-grained granular ice, the critical confining pressure was considered to be, at most, 10 MPa at strain rates below $1 \times 10^{-2}\text{ s}^{-1}$ and about 20 MPa at $5 \times 10^{-2}\text{ s}^{-1}$.

Parts A and B of Figure 2 show typical stress strain curves at $2 \times 10^{-3}\text{ s}^{-1}$ for coarse-grained granular and columnar ice loaded along the columnar grains, respectively, for various confining pressures. In the tests for columnar ice, the major load was applied either along or across columnar grains. We did not observe significant differences between loading directions in strength and failure mode for confining pressures above 5 MPa. It is clear on comparing the curves for a confining pressure of 10 MPa that the effects of confining pressure on fracture mode and strength vary with crystal texture. The coarse granular ice behaved in a ductile manner, while the columnar ice fractured brittly. Maximum strength at this strain rate was attained at 5 MPa for coarse granular ice and at 10 MPa for columnar ice. This means that the critical confining pressure for a given strain rate is strongly influenced by crystal texture. The stress–strain relations at $2.5 \times 10^{-2}\text{ s}^{-1}$ for coarse-grained granular and columnar ice (loaded across columnar grains) are shown in parts C and D of Figure 2, respectively. As can be seen in this figure, a confining pressure of 50 MPa barely suppressed brittle failure for coarse-grained granular ice, while for columnar ice the confining pressure was insufficient to suppress brittle failure and there is little difference in fracture stress for confining pressures of 10 and 50 MPa. The figure

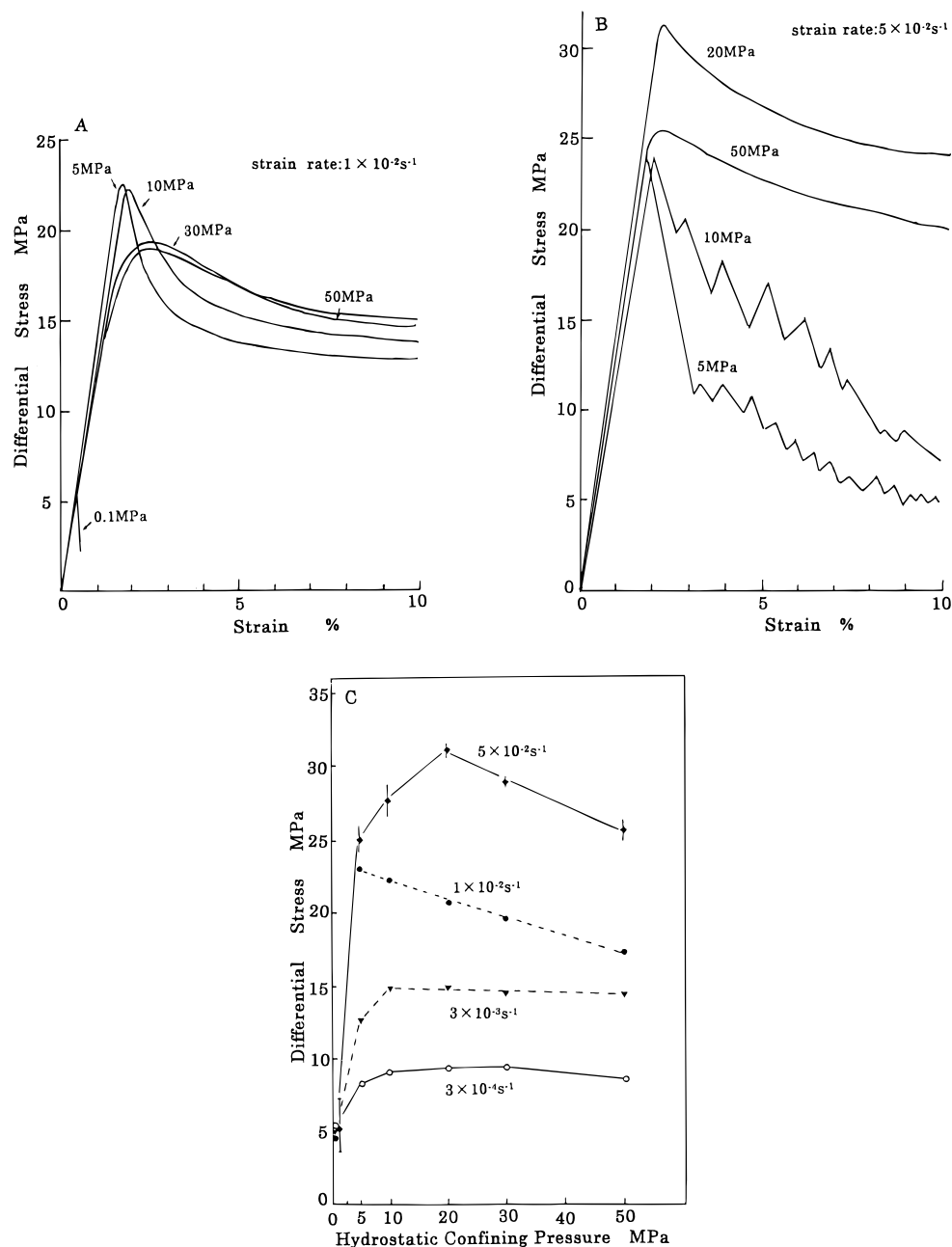


Figure 1. Stress–strain curves for fine-grained granular ice for various confining pressures at strain rates of $1 \times 10^{-2} \text{ s}^{-1}$ (A) and $5 \times 10^{-2} \text{ s}^{-1}$ (B). Compressive yield/fracture stress of fine-grained granular ice as functions of strain rate and confining pressure (C).

shows that the compressive stress for brittle failure is not always dependent on the amount of confinement, but the strain at the peak stress increased and the number of repetitive rises and drops in stress within a certain strain range decreased with increase in confining pressure. At lower strain rates, the maximum stress for a given strain rate is found at the critical confining pressure. On the other hand, at high strain rates, where brittle failure alone occurs, the strength is strongly affected by the manner of failure, such as axial splitting, shear failure with a single slip plane or with multiple slip planes, or an extended slip band with microcracking and granulation.

4.2. Thin Section. After completion of each test and a general inspection of the deformation or fracture mode and crack pattern in the specimen, a thin section was prepared to determine if there was any correlation between the deformation behavior and the change in the internal structure. The thin sections shown in Figure 3A,B,C are from fine-grained samples compressed at

$5 \times 10^{-2} \text{ s}^{-1}$ to a strain of about 10% under confining pressures of 5 MPa (A,B) and 20 MPa (C). The associated stress–strain relations are shown in Figure 1B. Figure 3A is parallel to the major stress and 3B is perpendicular to it. The crystal texture of the sample, which fractured by brittle shear with a single slip plane, suffered little change except in the region of the slip plane. Figure 3C is a thin section from a specimen deformed under a confining pressure of 20 MPa, for which the deformation was ductile. The texture was significantly changed by granulation throughout the specimen. The granulation is thought to be due to microcracking because the whole body appeared to be opaque.

The effect of the confining pressure on the crystal texture of coarse granular ice is shown in Figure 3D,E,F. The associated stress–strain curves are shown in Figure 2C. For thin sections, Figure 3D,E, shear failure occurred under a confining pressure of 5 and 10 MPa, respectively. For a confining pressure of 5 MPa failure occurred in a single plane and little change in texture

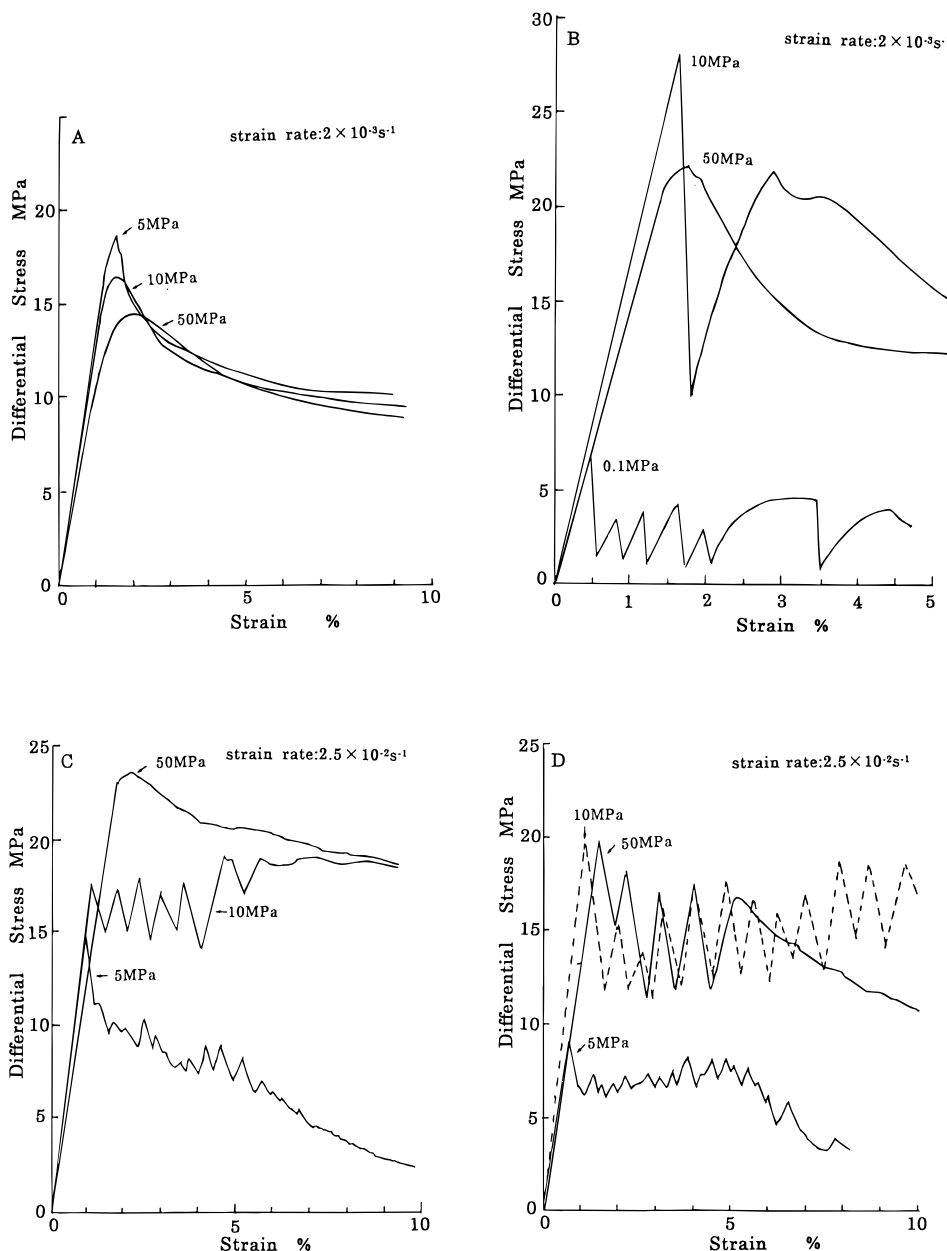


Figure 2. Stress-strain curves at $2 \times 10^{-3} \text{ s}^{-1}$ for various confining pressures for coarse-grained granular ice (A) and columnar ice loaded along columnar grains (B), and at $2.5 \times 10^{-2} \text{ s}^{-1}$ for coarse grained ice (C) and columnar ice loaded across columnar grains (D).

was associated with it (Figure 3D). On the other hand a confining pressure of 10 MPa (Figure 3E) caused the shear failure to be more extensive, with larger regions of slip and granulation. The confining pressure of 50 MPa (Figure 3F) caused microcracking and granulation to be more general, resulting in ductile deformation behavior.

5. Discussion and Conclusion

Our results on the relation between confining pressure and compressive strength confirmed the previous work by Jones⁶ for fine-grained granular ice and had tendencies similar to the results of Rist and Murrell⁹ and Kalifa et al.⁷ conducted under hydrostatic confining pressure.

The critical confining pressure for the brittle to ductile transition was strongly influenced by crystal texture as well as strain rate. The dependence of the critical confining pressure on crystal texture is attributed not only to the dependence of initial crack formation on grain size, strain, and stress shown by Kalifa

et al.,¹³ but also to the initial crack size, which can be considered to be equivalent to grain size. Thin sections revealed that cracks formed predominantly in the planes of maximum shear, generally inclined at 45° to the maximum stress under a confining pressure. Crack formation within a certain strain range increases with increasing strain rate or stress until brittle failure occurs. As the confining pressure acts against frictional slip between crack surfaces, it suppresses crack growth to the critical size required for brittle fracture. Assuming the size of an initial crack is the same order as grain size, the confining pressure required to suppress crack growth to the critical size for brittle fracture must increase as grain size increases. Accordingly the dependence of the critical confining pressure on crystal texture is considered to be due to the initial crack size.

The examination of the correlation between the microprocess and the failure mode and of the dependence of the effect of hydrostatic confining pressure on crystal texture has led to the following conclusions.

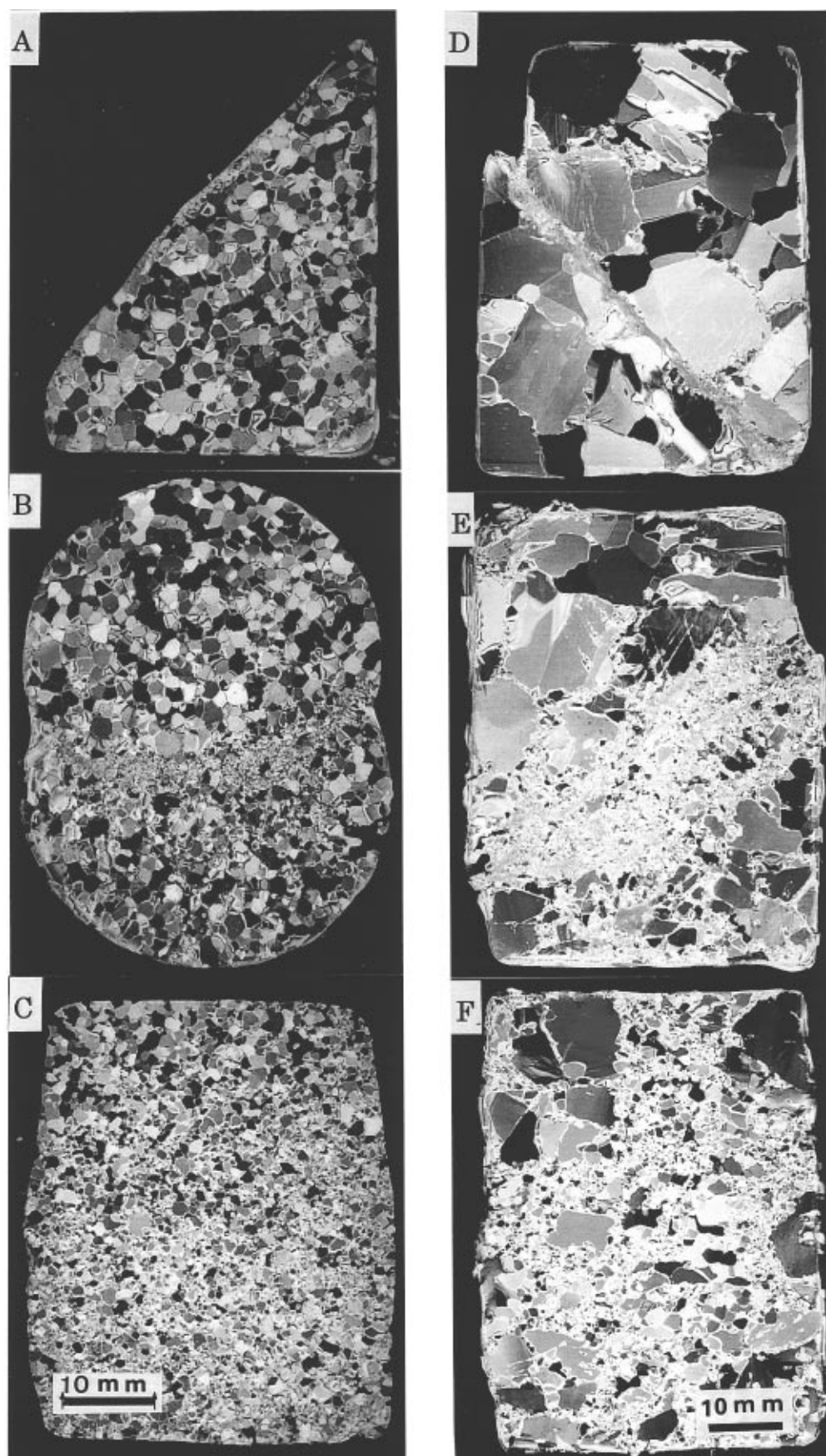


Figure 3. Thin sections of fine-grained granular ice deformed to a strain of 10% at $5 \times 10^{-2} \text{ s}^{-1}$ under confining pressures of 5 MPa (A, B) and 20 MPa (C). Thin sections of coarse-grained granular ice deformed to a strain of 10% at $2.5 \times 10^{-2} \text{ s}^{-1}$ under confining pressures of 5 MPa (D), 10 MPa (E) and 50 MPa (F).

The strength increased to a maximum with increasing confining pressure up to a critical value at which a brittle to ductile transition occurs. The critical confining pressure increased with increase in strain rate and grain size. For fine-grained granular ice, a confining pressure of 20 MPa caused the ice to behave in a ductile manner, even at a strain rate of $5 \times 10^{-2} \text{ s}^{-1}$, and the yield strength to reach 30 MPa. Application of a confining pressure above 20 MPa caused fine-grained ice to deform in a ductile manner for all strain rates applied; a confining pressure of 50 MPa was required at $2.5 \times 10^{-2} \text{ s}^{-1}$ for coarse-grained granular ice and $1 \times 10^{-2} \text{ s}^{-1}$ for columnar ice.

The failure mode changed from shear fracture with a single slip plane to that with multiple slip planes or extended shear zone and to pseudoductile, with increasing confining pressure. Crystal texture was changed mainly by granulation, which was caused by crack formation. Change in crystal texture was remarkable along macroscopic fracture zones for brittle fracture and in specimens deformed in a ductile manner at high strain rate and high confining pressure.

Acknowledgment. The author expresses her grateful thanks to emeritus Prof. Y. Suzuki of the Institute of Low Temperature

Science, Hokkaido University, for designing the high-pressure cell. Thanks are also due to Messrs. K. Shinbori, T. Segawa, H. Ishii, S. Matsumoto, and S. Nakatsubo for technical help and to Mr. Y. Kamata for help with the experiment, as well as to Messrs. A. Sasaki and K. Itoh for controlling the temperature of a cold room and maintenance. The rubber jacket was offered by Kyowa Co., Ltd., in Osaka.

References and Notes

- (1) Schulson, E. M. *Acta Metall. Mater.* **1990**, *38*, 1963.
- (2) Gold, L. W. *J. Glaciol.* **1977**, *19*, 197.
- (3) Heafeli, R.; Jaccard, C.; deQuervain, M. I.U.G.G. General Assembly of Bern, IAHS Publ. No. 79, **1968**; p 341.
- (4) Jones, S. J.; Chew, H. A. M. *J. Phys. Chem.* **1983**, *87*, 4064.
- (5) Mizuno, Y. High-temperature creep of polycrystalline ice under hydrostatic pressure. In *Physics and Chemistry of Ice*; Maeno, N., Hondoh, T., Eds.; Hokkaido Univ. Press: Sapporo, Japan, **1992**; p 434.
- (6) Jones, S. J. *J. Glaciol.* **1982**, *28*, 171.
- (7) Kalifa, P.; Ouillon; Duval, P. *J. Glaciol.* **1992**, *38*, 65.
- (8) Rist, M. A.; Jones, S. J.; Slade, T. D. *Ann. Glaciol.* **1994**, *40*, 305.
- (9) Rist, M. A.; Murrell, S. A. F. *J. Glaciol.* **1994**, *40*, 305.
- (10) Schulson, E. M.; Jones, D. E.; Kuehn, G. A. *Ann. Glaciol.* **1991**, *15*, 216.
- (11) Smith, T. R.; Schulson, E. M. *Acta Metall. Mater.* **1993**, *41*, 153.
- (12) Weiss, S. J.; Schulson, E. M. *Acta Metall. Mater.* **1995**, *43*, 2303.
- (13) Kalifa, P.; Jones, S. J.; Slade, T. D. *Ann. Glaciol.* **1991**, *15*, 222.